INTERNATIONAL JOURNAL OF TECHNO-ENGINEERING
IJTE

ISSN: 2057-5688

Power Quality Improvement in a PV Based EV Charging Station Interfaced with Three Phase Grid

Dr.N Lakshmi Narayana [1], M Sivanageswara rao [2], G Ravi Kumar [3]
[1] professor, [2]Associate Professor, [3] Assistant professor
Department of Electrical and Electronics Engineering
Priyadarshini Institute of Technology & Science, Tenali,Guntur

***Abstract*— This paper deals with the power quality improvement in a solar photovoltaic (PV) array generation-based EV (Electrical Vehicle) charging station. The EV battery can be charged using the power produced by a PV array when the charging station is used independently. Additionally, it communicates with the utility and supplies it with the remaining electricity. The adjustment of reactive power for the enhancement of grid power quality is another benefit of the charging station. The following are the functions of the charging station. Harmonics current compensation, control over EV battery charging and discharging, simultaneous EV battery charging and harmonics current compensation, and simultaneous EV battery discharging and harmonics current compensation are the four main components. The charging station is managed to provide excellent performance even when the mains voltage is imbalanced, keeping the total harmonic distortion of the mains current below 5% as recommended by the IEEE 519 standard. Thanks to careful design of the control strategy, the charging station operates in grid-connected mode. However, the charging station works in standalone mode and the PV array charge the EV batteries when out of sync. In addition, a synchronous control is created to connect the system to the grid as soon as it becomes available.**

Keywords— EV charging station, DC-DC bidirectional converter, power quality, solar photovoltaic, VSC

I. INTRODUCTION

Concerns over pollution and resource depletion have increased the popularity of electric vehicles (EVs) [1]. The increasing demand for electric vehicles necessitates the installation of charging stations. Electric vehicle batteries are normally charged by utility power. [2-4] present grid-based charger topologies for charging EV batteries. These topologies require large amounts of grid power to charge the EV batteries. On the other hand, the charger's unidirectional current flow architecture prevents the actual current from flowing backwards from the car to the grid. EV batteries can be used as a kind of energy storage to harness power when demand is high [5]. Overwhelming majority. Most of the time, electric cars are parked with a large amount of energy stored. It's an electric car when not in use, the grid receives power from the battery to cover peak demand. To do this, the electric vehicle charger must allow bidirectional active power flow [6]. The way electric vehicles send power to the grid is known as "Vehicle to Grid" (V2G). In this mode, EV charging is capable of providing reactive power support to the grid [7-10]. Supports reactive power near the end of the load [9]. PV disruption is eliminated by using EV batteries as buffer storage and connecting charging stations to the grid [10, 11]. Demonstrated the effectiveness of on-board charging in charging EV batteries.

Batteries with low power consumption, on the other hand, are charged on board. As such, off-board chargers are a more practical choice than on-board chargers. [12–13] Examine the off-board charger topology. Current research envisions a single-stage, solar-powered, off-board charging station for grid-connected electric vehicles. This outlet allows power to flow in both directions. A bi-directional converter connects the electric vehicle to his DC intermediate circuit at the charging station. Bi-directional converters protect EV batteries from second harmonic currents and DC link ripple, extending battery life. Furthermore, the battery performance of electric vehicles is no longer determined by the intermediate circuit voltage. The bidirectional converter's duty cycle controls battery charging and discharging.

PV arrays are used to charge electric vehicle (EV) batteries, sending additional power to the utility company, alleviating the need for generators. The VSC provides the required reactive power regulation for the grid. Connecting

INTERNATIONAL JOURNAL OF TECHNO-ENGINEERING
IJTE
ISSN: 2057-5688

solar-powered EV charging stations to the grid improves the quality of the grid power supply. It operates independently in grid failure mode to generate power for the PV array and charge the EV batteries. The system is also evaluated under various dynamic conditions, such as: B. Fluctuations in photovoltaic solar radiation, grid voltage imbalance, and changes in reactive power in the grid. The charging station will sync with the network when restored. Active and reactive power reference instructions are used in the charging station control architecture. Electric vehicle owners use the reference active power command to determine whether to charge or discharge the electric vehicle battery. The reference reactive power is selected according to the inductive/capacitive reactive power parameters required for continuous operation of the charging station.

Charging stations are configured so that electric vehicle owners can choose their own charging and discharging times. System operation when mains power is needed to charge an EV battery, it is called G2V (Grid to Vehicle). The system is called V2G (Vehicle to Grid), in which the battery of an electric vehicle discharges to power the grid. Depending on the situation, the charging station can also adjust reactive power (delay/lead).

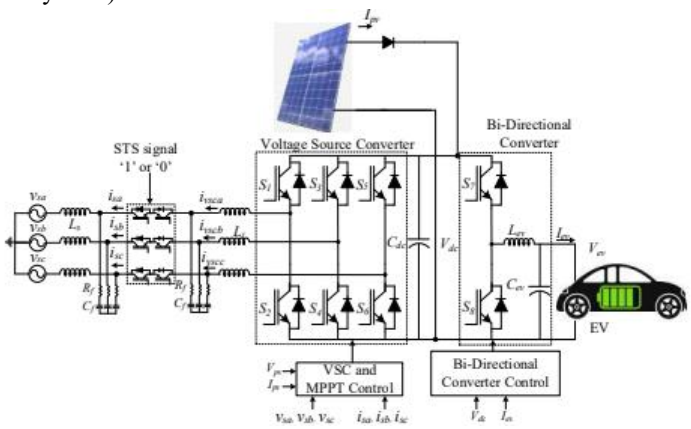

Fig. 1 Three-phase PV system with an EV and three wires that is connected to the grid

II. SYSTEM CONFIGURATION

A block design of a single-stage PV-based EV charging station is shown in Figure 1. Direct current produced by PV arrays is used to charge electric vehicle batteries at PV-based charging stations. Electric car batteries are charged and discharged using bi-directional converters. The PV generator is directly linked to the intermediary circuit. As a result, the charging station's total cost is decreased and the requirement for a boost converter is removed. To convert DC to AC, which may be linked to the grid, IGBT-based VSCs are employed. An IGBT-based switch called a static transfer switch is used to link a charging station to the electrical grid.

To increase the collecting capacity of charge carriers created by photonics, the p-n connections of the emitter and base sub boxes are situated very near the surface. The thin emitter sub layer of the junction has a rather high resistance, which makes it difficult to design a useful contact grid. The pictures show this. A number of crystalline Si cells are connected in series either above or below a thin film layer to create solar cell modules. He has two roles in this module. It protects the solar cell from the bottom up and produces a higher voltage compared to a single solar cell, which can only produce less than 1 volt. The module edge is a bit lower than the instantaneous product cell's conversion edge, which is between 13 and 16. The maximum crystalline silicon efficiency that has been determined in a lab to date is 24.7, which is very near to the figure anticipated for this type of solar cell. The process of photoelectric conversion does not simply involve semiconductors and p-n junctions. There could be a huge number of new concepts and features developed in the future.

III. CONTROL SCHEME

The Present-day charging stations' primary function is to provide PV array electricity for EV charging. The solar system may be used to power the charging station, which is wired into the electrical grid. Electric cars also have the ability to both use and provide energy to the grid. Intelligent control systems must be constructed to make better use of charging stations. The developed control technique is depicted in Figure 2. The controller only recognises two input instructions overall.

A. Active Power Reference Command

This decision depends on whether the electric vehicle battery needs to be charged or discharged. EV owners can choose to charge or discharge their EV batteries to power the grid. They are then urged to sell electricity to the grid during periods of high demand.

B. Reactive Power Reference Command

Regardless of whether the reactive power is capacitive or inductive in form, it is controlled in terms of both quantity and kind. There are two types of controls for EV charging stations: independent mode control and VSC and EV charge/discharge control in combination with grid control.

INTERNATIONAL JOURNAL OF TECHNO-ENGINEERING
IJTE
ISSN: 2057-5688

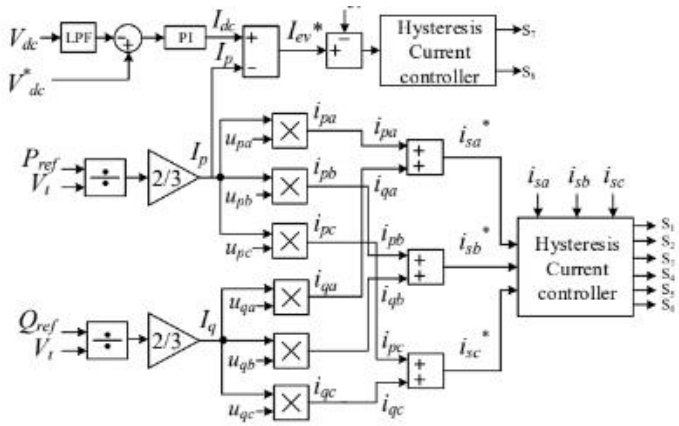

Fig. 2 Controller diagram

Both active and reactive power reference commands are required to generate VSC switching pulses in grid-tied mode of operation. An EV battery must be charged and discharged under control, which calls for a bidirectional DC-DC converter. The next part goes into more depth about the control system.

C. VSC Control in Grid Connected Mode

The grid-coupled nature of VSC gate pulse production is seen in Figure 2. The active and reactive parts of the current are each contributed to by Pref (active power reference command) and Qref (reactive power reference command), respectively. Multiplying the active component of the current (Ip) by the common-mode unit template (upa, upb, and upc) yields the active current per phase (ipa, ipb, and ipc). The quadrature unit templates (uqa, uqb, and uqc) are multiplied by the reactive component of the current (Iq) to determine the reactive currents (iqa, iqb, and iqc) for each phase. The next section goes into great depth about controls.

1) In-phase and quadrature-phase estimation

Unit Templates (UTs) and Terminal Voltage Amplitude (TVA) Figure 3 depicts a calculation of the PSCs [14] for the grid voltages when they are out of balance. The voltage at the terminal amplitude is approximated using the PSCs in the following manner:

$$V_t = \sqrt{\frac{2}{3} \times \left(v_{pa}^2 + v_{pb}^2 + v_{pc}^2\right)} \quad (1)$$

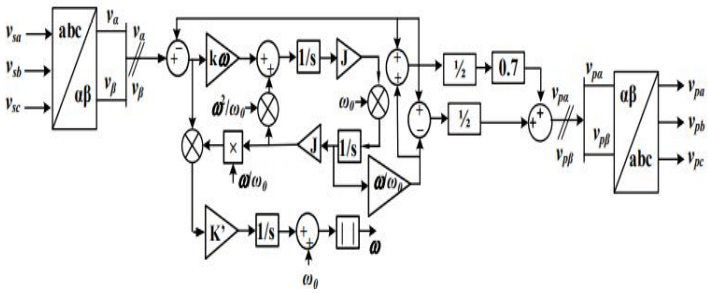

Fig. 3 estimating grid voltages in the positive sequence

The expected in-phase UTs are

$$u_{pa} = \frac{v_{pa}}{V_t}, u_{pb} = \frac{v_{pb}}{V_t}, u_{pc} = \frac{v_{pc}}{V_t} \quad (2)$$

The quadrature phase UTs are determined in the same way as,

$$u_{qa} = -\frac{u_{pa}}{\sqrt{3}} + \frac{u_{pc}}{\sqrt{3}}, u_{qb} = -\frac{\sqrt{3}u_{pa}}{2} + \frac{(u_{pb}-u_{pc})}{2\sqrt{3}} u_{qc} = -\frac{\sqrt{3}u_{pa}}{2} + \frac{(u_{pb}-u_{pc})}{2\sqrt{3}} \quad (3)$$

Using the quadrature phase and in-phase UTs obtained in (2) and (3), the corresponding reference grid currents (isa *, isb *, and isc *) that synchronise with the reference grid phase voltages (vsa *, vsb *, and vsc *) are estimated.

2) Estimation of Grid Currents Active Components

The active and reactive components of the mains current determine the amplitude of the mains current, the mains voltage and the phase difference. The grid current active component (Ip) is used to display the current electrical power flowing through the charging station. This component can be roughly calculated as follows using the power that is active reference command (Pref) and the terminal voltage amplitude:

$$I_p = \frac{2}{3} * \frac{P_{ref}}{V_t} \quad (4)$$

If the active component of the grid current (Ip) is positive, EV batteries charge; otherwise, they drain.

3) Grid Currents Reactive Component Estimation

The reactive component of the grid current (Iq) representing the exchange of reactive power. It is calculated as follows using the terminal voltage amplitude and reactive power reference (Qref).

$$I_q = \frac{2}{3} * \frac{Q_{ref}}{V_t} \quad (5)$$

4) Grid Reference Currents Computation

The The actual components and unpolished ingredients (IP and IQ) of the main power supply current are used to

INTERNATIONAL JOURNAL OF TECHNO-ENGINEERING
IJTE
ISSN: 2057-5688

calculate the same phase components of the standard power supply current and the right angle phase component. These components are used to calculate the grid reference current in the following manner.

$$i_{sa}^{*} = i_{pa} + i_{qa}, i_{sb}^{*} = i_{pb} + i_{qb}, i_{sc}^{*} = i_{pc} + i_{qc} \quad (6)$$

where the in-phase and quadrature components of the reference line current, respectively, are denoted by ipa, ipb, ipc, iqa, iqb, and iqc. These factors are determined as follows:

$$i_{pa} = I_P \times \mathrm{u}_{pa}, i_{pb} = I_P \times \mathrm{u}_{pb}, i_{pc} = I_P \times \mathrm{u}_{pc}$$
$$i_{qa} = I_q \times \mathrm{u}_{qa}, i_{qb} = I_q \times \mathrm{u}_{qb}, i_{qc} = I_q \times \mathrm{u}_{qc} \quad (7)$$

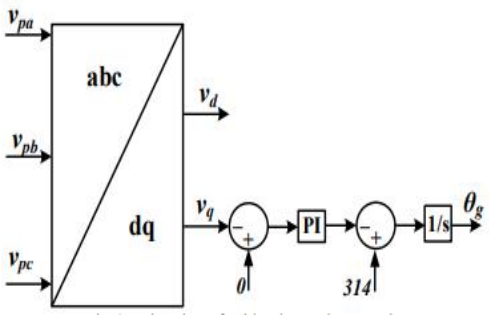

Fig. 4 Grid voltage phase angle estimation

The sense grid currents (isa, isb, isc) are subtracted from the reference grid currents (isa*, isb*, isc*) and fed to a hysteresis current controller to generate the VSC gate pulse.

D Standalone Mode and Synchronization

During the power outage, control of the changing station changes to standalone mode. When comparing the phase angles of the grid voltage and PCC voltage (g and s), the error is determined as,

$$\theta_e(k) = \theta_g(k) - \theta_s(k) \quad (8)$$

Where

The PI controller receives this error in order to determine the frequency error as shown in Fig. 4.

$$\Delta\theta_d(k) = \Delta\theta_d(k-1) + - k_{ps}\{\theta_e(k) - \theta_e(k-1)\} + \theta_{is}\{(\theta_e(k))\} \quad (9)$$

Where,

kps and kis are PI controller gains coefficients.

The new phase angle θn is calculated as follows:

$$\theta_n(k) = \theta_s(k) + \Delta\theta_d(k) \quad (10)$$

In standalone mode, the PCC phase voltage (Vts) peak amplitude is used by VSC to generate a sinusoidal reference voltage as follows:

$$v_{vsca}^{*} = V_{ts} \sin(\theta_n)$$
$$v_{vsca}^{*} = V_{ts} \sin(\theta_n - 120^0)$$
$$v_{vsca}^{*} = V_{ts} \sin(\theta_n - 240^0) \quad (11)$$

Where,

The phase reference angle is n, and Vts is equal to 2302/(3 V). By integrating the reference angular frequency, it is evaluated. The reference voltages produced in (1) are then compared to the sensed phase voltages, and the voltage errors (vea, veb, and vec) are sent to the PI controller.

$$i_{vsca}^{*} = i_{vsca}^{*}(k-1) + k_{pv}\{v_{ea}(k) - v_{ea}(k-1)\} + k_{iv}\{v_{ea}(k)\} \quad (12)$$

$$i_{vscb}^{*} = i_{vscb}^{*}(k-1) + k_{pv}\{v_{eb}(k) - v_{eb}(k-1)\} + k_{iv}\{v_{eb}(k)\} \quad (13)$$

$$i_{vscc}^{*} = i_{vscc}^{*}(k-1) + k_{pv}\{v_{ec}(k) - v_{ec}(k-1)\} + k_{iv}\{v_{ec}(k)\} \quad (14)$$

The hysteretic current controller may supply switching pulses to VSC by comparing the recorded reference current to the measured PCC current.

INTERNATIONAL JOURNAL OF TECHNO-ENGINEERING
IJTE
ISSN: 2057-5688

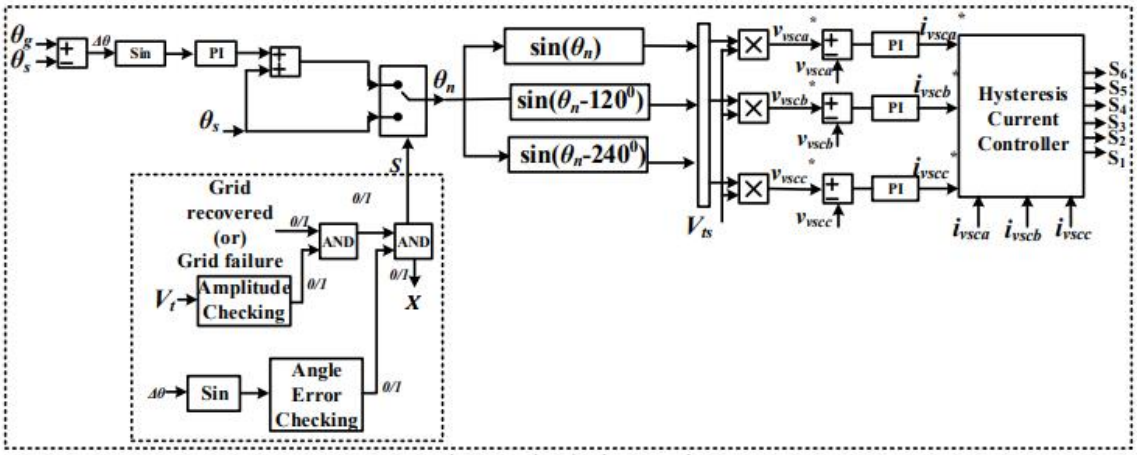

Fig. 5 Synchronization control

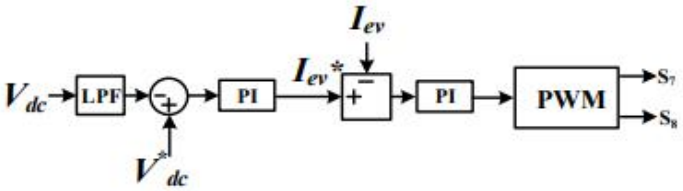

Fig. 6 In standalone mode, control of EV charging and discharging

The controller synchronizes the grid voltage (vs) with the PCC voltage (vvsc) just before reconnecting to the grid when the grid recovers from the island condition. Figure 5 shows synchronous control. Line frequency (fs), electric field (e), and voltage amplitude (Vt) are variables that control the operating mode of the system. The grid is cut off from the rest of the system and pushed into island mode when the grid voltage amplitude (Vt > 1.1 pu or Vt 0.88 pu), the phase angle g s, or the grid frequency (fs > 50.5 Hz or fs 49.5 Hz) at the PCC becomes anomalous or out of range. According to Figure 5, the synchronous controller sends a "1" (on) or "0" (off) signal to the STS depending on whether the system is running in grid-tied mode or island mode using these voltage and frequency characteristics.

E. EV Charging/Discharging Control in Standalone Mode

The DC link voltage (Vdc*), which is derived via MPPT, acts as a reference to maintain the DC link voltage under dynamic situations. The DC link voltage is always maintained constant thanks to the controller's architecture, preventing voltage variations throughout the charging and discharging of the electric car. Each time, a predetermined amount of power is swapped with the grid, saving the grid from having to work harder. The reference grid current is estimated to be at

$$I_{ev}^{*} = I_{dc} - I_{p} \qquad (15)$$

Where

Idc maintains Vdc*, the DC-link voltage, as constant. This Idc is determined by subtracting the measured DC-link voltage from Vdc* and using a PI controller to pass the error produced:

$$I_{ev}^{*} = \left(k_{pd} + {}^{k_{id}}/_{S}\right)\{V_{dc}^{*} - V_{dc}\} \qquad (16)$$

Where

Kpd and Kid are the gain coefficients for the PI controller. The bi-directional converter's gating pulses are produced by the PI controller after the battery reference current (Iev *) and EV current have been compared, as shown in Fig. 6.

IV RESULTS AND DISCUSSION

A typical solar panel might be able to provide an electric car with enough energy for a longer range by charging the battery when it is stationary and in motion. It might help with problem-solving. This essay shows how incorporating photovoltaic (PV) modules might extend the range of electric vehicles. Models were created and tested using MATLAB/Simulink terrains. The results show that the PV module can charge the battery to the appropriate level. An energy benefit analysis was also conducted to demonstrate the energy savings achieved and the benefits provided by the solar-powered grounded electric vehicle.

A Response of Charging Station at Steady State

INTERNATIONAL JOURNAL OF TECHNO-ENGINEERING
IJTE
ISSN: 2057-5688

Voltages and currents for a three-phase network are shown in Figure 8. The three-phase line currents are 4.987 A, 5.155 A, and 5.072 A, respectively, while the three-phase line voltages are 213.37 V, 216.99 V, and 214.70 V. This is an illustration of the sinusoidal balancing of the mains current. The power factor is displayed on a graph. Since 8 equals 0.9978, it is quite near to 1. The 1.885 kW of power that the PV system sends to the grid is shown in Figure 10.

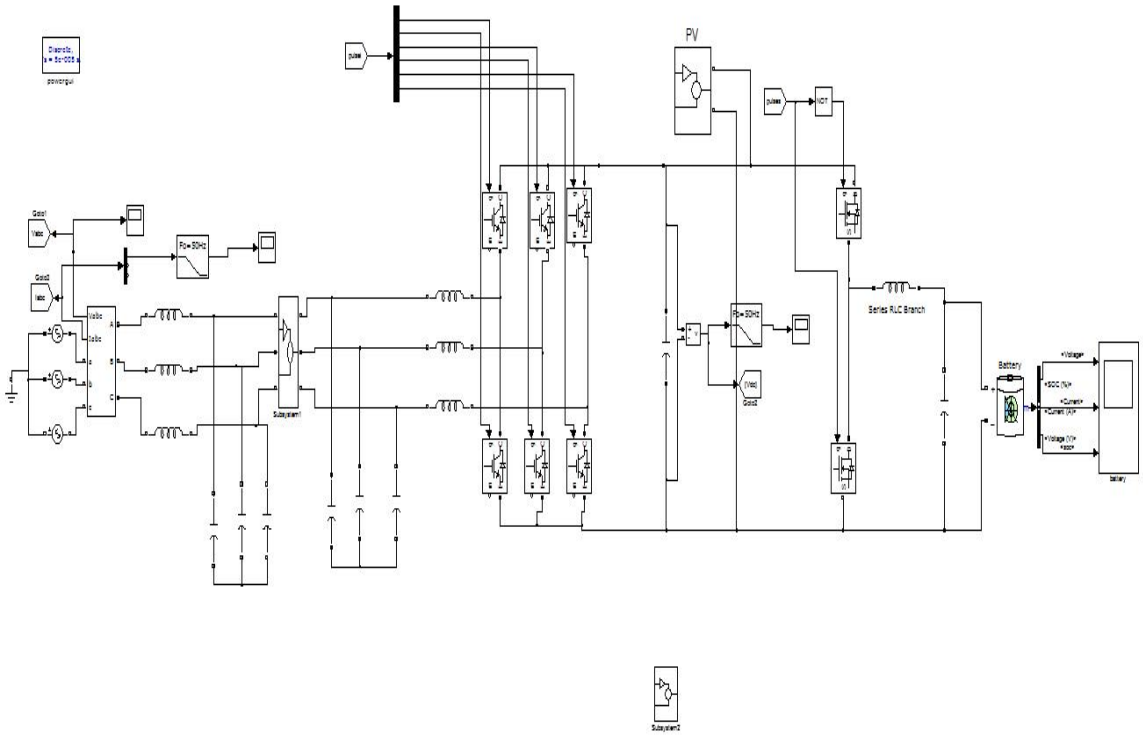

Fig. 7 circuit diagram

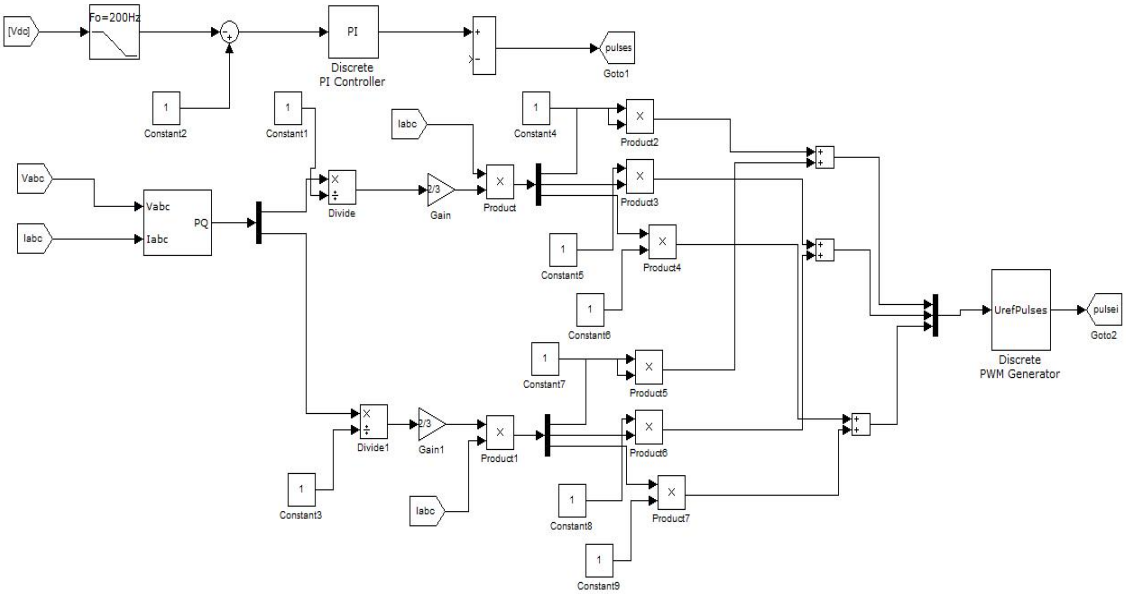

ISSN: 2057-5688

Fig. 8 control circuit

INTERNATIONAL JOURNAL OF TECHNO-ENGINEERING
IJTE
ISSN: 2057-5688

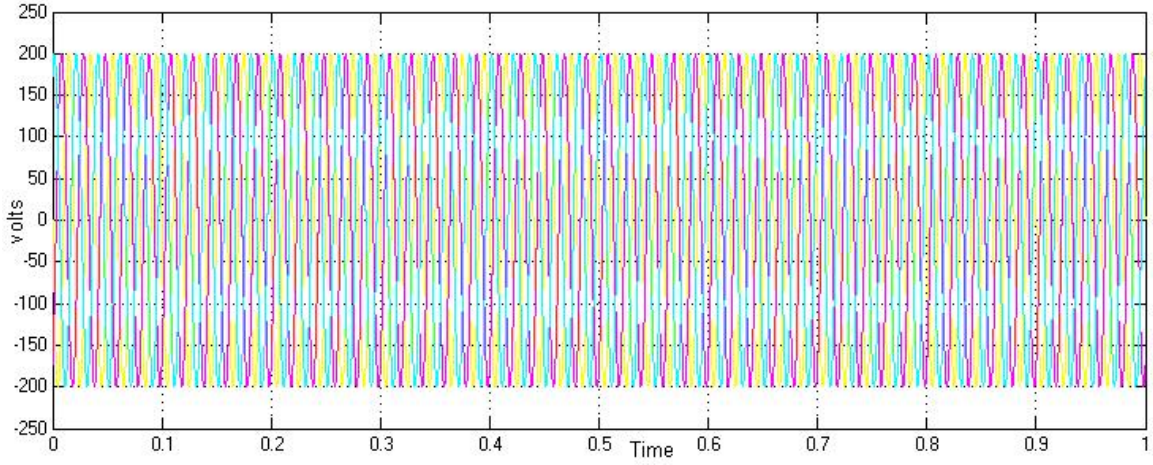

Fig. 9 Source voltage

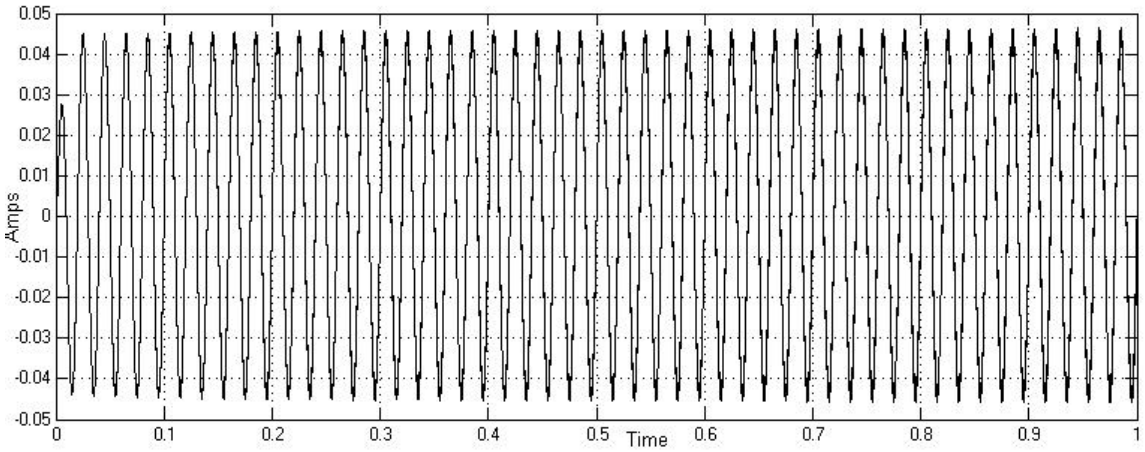

Fig. 10 Source current

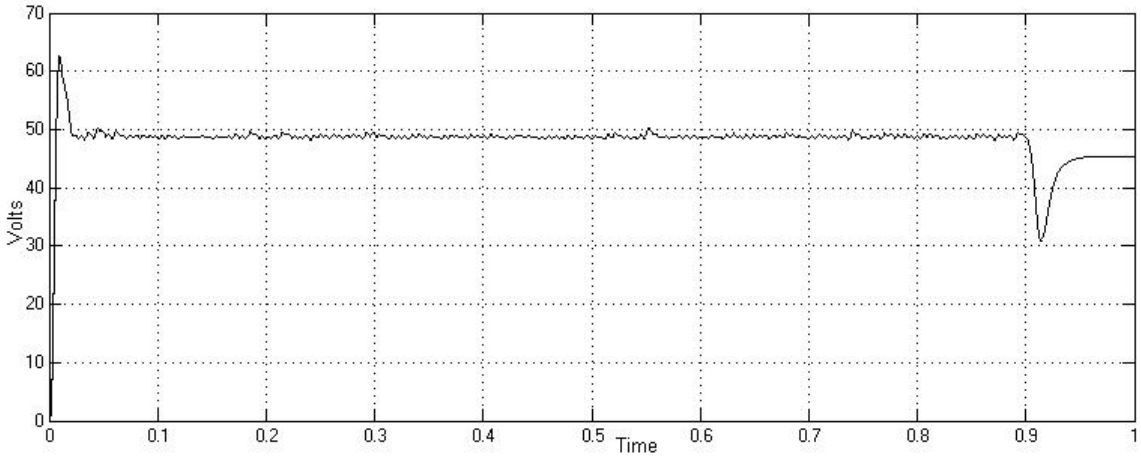

Fig. 11 Capacitor Voltage

ISSN: 2057-5688

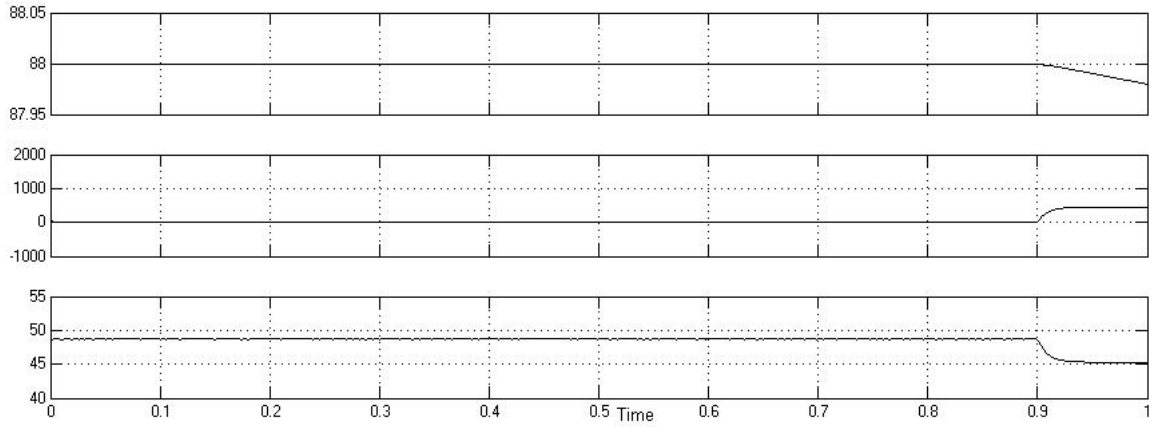

Fig. 12 battery ratings

Energy supply reduces as solar radiation rises. The grid then adjusts for the energy dip, keeping the PV voltage, DC link voltage, and EV current constant. As a result, the PV system's current is running less. The performance of the charging station is depicted in Figure 12 as the PV solar irradiation rises. More electricity is produced as the PV generator's current rises in response to rising solar radiation. Power that is not used by the EV is returned to the grid when it charges at a consistent rate. On the other hand, if the EV current is constant, the PV voltage and intermediate circuit voltage stay constant. As seen in Figure 6.4, when the grid is operating in constant power mode and PV insolation rises, EVs use extra electricity to charge more quickly. Since the VSC always feeds the grid and the EV charging rate rises, neither the VSC power nor the grid power changes. The grid will adjust the backup power and grid current will rise when solar radiation rises and the grid voltage becomes unstable.

V CONCLUSION

A grounded, single-stage solar-powered EV charging station that is connected to the grid, feeds the power produced there to the grid, and delivers the EV's batteries to the grid to release power during peak hours is being constructed. You stand to gain. The charging station receives reactive power compensation after being wired into the electrical grid. The grid connection and freestanding modes of operation both operate satisfactorily, according to the charging station capacity evaluation. The charging station syncs with the grid, feeding more power into the grid when the grid is operating efficiently. The charging station functions admirably under dynamic circumstances like varying solar insolation, erratic grid voltage, and reactive power regulation, according to experimental data.

FUTURE SCOPE

Analysts predict that the number of charging stations will increase over the next five years due to the expected rapid growth of EVs (500,000 stations by 2030). The global market for EV charging stations is expected to reach $30.41 billion by 2023.

REFERENCES

[1] M. Shatnawi, K. B. Ali, K. Al Shamsi, M. Alhammadi and O. Alamoodi, “Solar EV Charging,” Proc. 6. Inter. Renewable Energy Conference: Generation and Application (ICREGA), 2021, p. 178-183.

[2] PP Nachankar, H.M. Suryawansi, P. Chaturvedi, D. D. Atkar, C. L. Narayana and D. Govind, “Universal off-board battery chargers for light and heavy duty electric vehicles,” Proc. IEEE Inter. Conference on Power, Drives and Energy Systems (PEDES), 2020, p. 1-6.

[3] PK Sahu, A. Patanik, A. K. Day, T. K. Mohapatra, “New Circuits for Battery Charging and Motor Control in Electric Vehicles,” Proc.1st Odisha Inter. Conference Power Engineering, Communication and Comparative Technology (ODICON), 2021, pp. 1-6.

[4] p. Rehlaender, F. Schafmeister, J. Böcker, "Interleaved Single-Stage LLC Converter Design Using Half- and Full-Bridge Topologies for Large Voltage Transfer Ratio Applications," IEEE Transaction Power Electronics, vol. 36. No. 9, S. 10065-10080, September

ISSN: 2057-5688

[5] B. Quispe, G. de A., Melo, R.K. Cardim, J.M. de S. Ribeiro, “Single-Phase Bidirectional PEV Charger for V2G Operation with Coupled Inductor-Cuk Converter,” Proc. 22 IEEE International Technical Conference (ICIT), 2021, S. 637–642.

[6] H. Heydari-doostabad and TM O'Donnell, "High Voltage Gain, Wide Range Bidirektional DC-DC Converters for V2G and G2V Hybrid Electric Vehicle Chargers," IEEE Transactions Industrial Electronics, Early Access.

[7] C Tan, Q. Chen, L. Zhang, and K. Zhou, “Frequency Adaptive Repetitive Control of a Three-Phase Four-Legged V2G Inverter,” IEEE Transactions on Transportation Electrification, Early Access.

[8] K. Lai and L. Zhang, "Sizing and Sizing of Energy Storage Systems in Military-Based Vehicle-to-Grid Microgrids," IEEE Transactions Industry Applications, vol. 57, Nr. 3, S. 1909-1919, Mai-Juni 2021.

[9] M.H. Meravan Jaromi, P. Deganian, M.R. Mousavi Kademi and M.Z. Jahromi, "Reactive Power Compensation and Power Loss Reduction through Optimal Capacitor Placement," Proc. IEEE Texas Power and Energy Conference (TPEC), 2021, pp. 1-6.

[10] M. J. Aparicio and S. Grijalva, “Economic assessment of V2B and V2G for an office building,” in Proc. 52nd North American Power Symposium (NAPS), 2021, pp. 1-6.

[11] A. S. Daniel and K. R. M. V. Chandrakala, “Design of an isolated onboard plug-in electric vehicle charger,” in Proc. 7th International Conf. on Electrical Energy Systems (ICEES), 2021, pp. 147-149.

[12] H. Rasool et al., “Design optimization and electro-thermal modeling of an off-board charging system for electric bus applications,” IEEE Access, vol. 9, pp. 84501-84519, 2021.

[13] S. Koushik and V. Sandeep, “Design and selection of solar powered off-board domestic charging station for electric vehicles,” in Proc. International Conference on Sustainable Energy and Future Electric Transportation (SEFET), 2021, pp. 1-6.

[14] X. He, H. Geng and G. Yang, “A generalized design framework of notch filter based frequency-locked loop for three-phase grid voltage,” IEEE Transactions Industrial Electronics, vol. 65, no. 9, pp. 7072- 7084, Sept. 2018.